Wavefront control for high contrast imaging

Exo-planet imaging workshop

Laurent Pueyo

Johns Hopkins University
Physics and Astronomy department

February 6, 2012

Outline

1. Context
2. Wavefront sensing
3. Wavefront control
4. Conclusions

Direct Imaging of exo-planets

Two approaches

At the camera of an instrument dedicated to imaging exo-planets optical artifacts look like planets. We can:

1. Remove them “coherently”, e.g making PSF core starlight photons interfere destructively with starlight photons scattered by optical errors: *wavefront control*.

Direct Imaging of exo-planets

Two approaches

At the camera of an instrument dedicated to imaging exo-planets optical artifacts look like planets. We can:

1. Remove them "coherently", e.g making PSF core starlight photons interfere destructively with starlight photons scattered by optical errors: *wavefront control*.
2. Calibrate them using *post-processing* and use this calibration to reveal planets.

Direct Imaging of exo-planets

Two approaches

At the camera of an instrument dedicated to imaging exo-planets optical artifacts look like planets. We can:

1. **Remove them "coherently", e.g making PSF core starlight photons interfere destructively with starlight photons scattered by optical errors: wavefront control.**
2. Calibrate them using *post-processing* and use this calibration to reveal planets.

Direct Imaging of exo-planets

Two approaches

At the camera of an instrument dedicated to imaging exo-planets optical artifacts look like planets. We can:

1. Remove them “coherently”, e.g making PSF core starlight photons interfere destructively with starlight photons scattered by optical errors: *wavefront control*.
2. Calibrate them using *post-processing* and use this calibration to reveal planets.

Purpose of this lecture: wavefront sensing and control

This lecture is **not** and exhaustive review of all the concepts / instruments that have been proposed / are being built to address this problem .
This lecture is an attempt to look at wavefront control from the angle of the post-processing.

Quasi-static speckles

Statement of the problem

1. Mirrors are not perfect.
2. These imperfections scatter light.
3. The structure of this scattered light changes with time and wavelength.

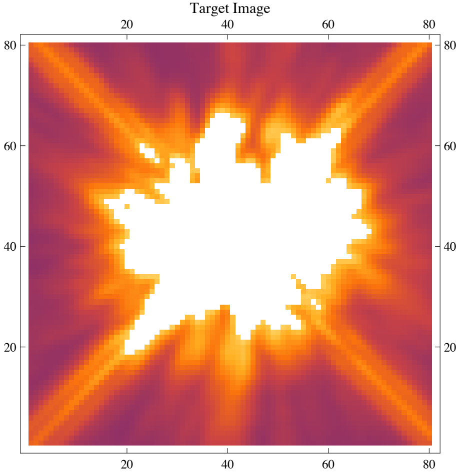

From Space: Two Hubble Space Telescope PSFs from two different rolls: the quasi-static speckles change a between the orientations.

Quasi-static speckles

Statement of the problem

1. Mirrors are not perfect.
2. These imperfections scatter light.
3. The structure of this scattered light changes with time and wavelength.

From Space: Two Hubble Space Telescope PSFs from two different rolls: the quasi-static speckles change a between the orientations.

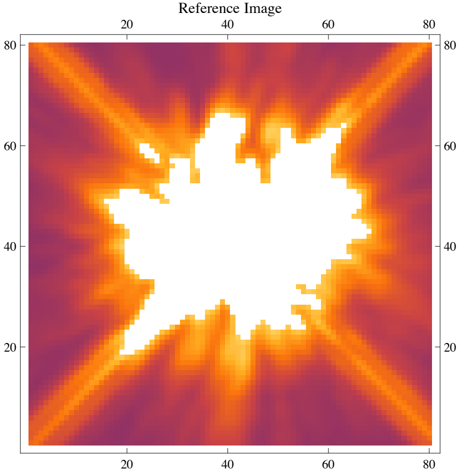

Quasi-static speckles

Statement of the problem

1. Mirrors are not perfect.
2. These imperfections scatter light.
3. The structure of this scattered light changes with time and wavelength.

From the ground: Project 1640 PSF.

- Diffuse halo due to the average atmospheric turbulence.

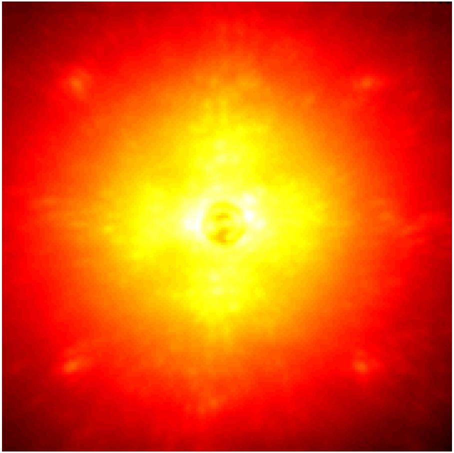

Quasi-static speckles

Statement of the problem

1. Mirrors are not perfect.
2. These imperfections scatter light.
3. The structure of this scattered light changes with time and wavelength.

From the ground: Project 1640 PSF.

- Diffuse halo due to the average atmospheric turbulence.
- Quasi-static speckles are present under the halo.

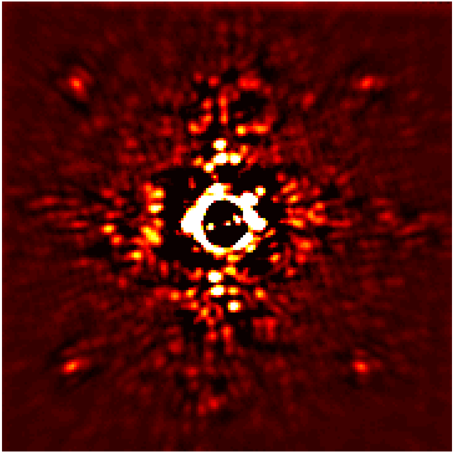

Quasi-static speckles

Statement of the problem

1. Mirrors are not perfect.
2. These imperfections scatter light.
3. The structure of this scattered light changes with time and wavelength.

From the ground: Project 1640 PSF.

- Diffuse halo due to the average atmospheric turbulence.
- Quasi-static speckles are present under the halo.
- Speckles vary slowly with time and wavelength.

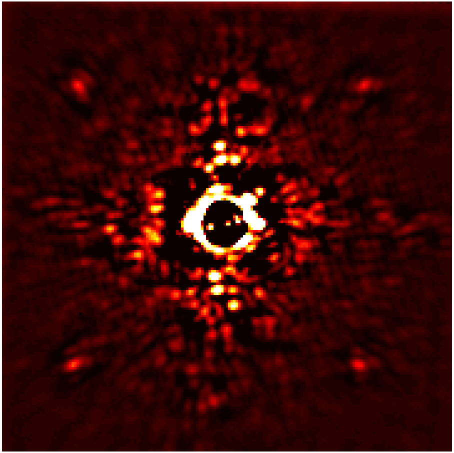

Quasi-static speckles

Crepp et al. (2010)

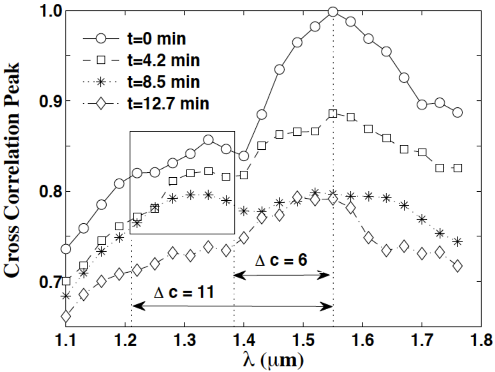

Quasi-static speckles decorrelate with time and wavelength.

Impact on post-processing

- In the absence of a good model of the PSF variations, this effect cannot be calibrated.
- Wavelength behavior can somewhat be predicted a priori.
- The time variations can be determined in the statistical sense.

Outline

1. Context
2. Wavefront sensing
3. Wavefront control
4. Conclusions

Wavefront sensing

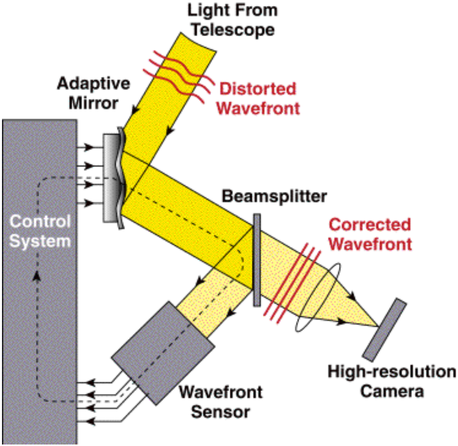

From Claire Max's lecture.

The wavefront actuation is done using a Deformable Mirror.
Cameras do not measure phase delays, they count photons. A wavefront sensor is an optical system which "converts" wavefront into images.

Wavefront sensing

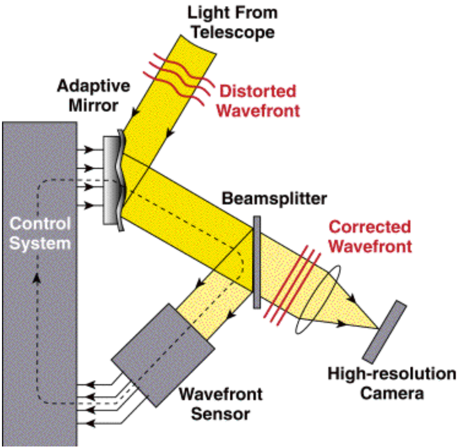

From Claire Max's lecture.

Wavefront sensing for Adaptive Optics

1. The order of magnitude of the errors is several waves.
2. The figure of merit is the Strehl ratio, or how much the PSF is concentrated in its core.
3. Non common path error are not critical under such a metric.

Wavefront sensing for High Contrast

1. The order of magnitude of the errors is < 1 wave.
2. The figure of merit is the actual contrast in the final image.

AO and wavefront control

Courtesy of B. Oppenheimer

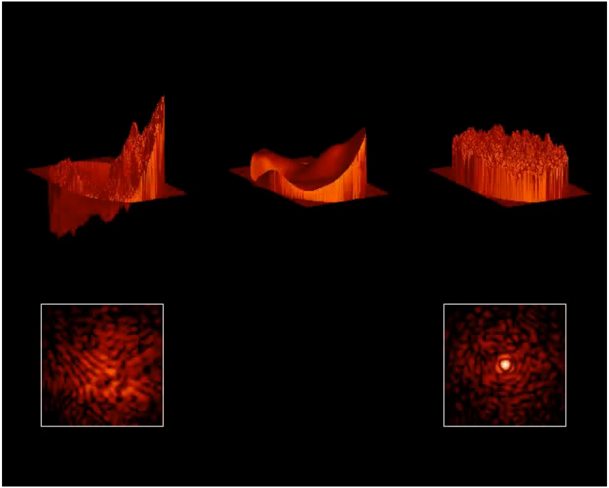

AO and wavefront control

Courtesy of B. Oppenheimer

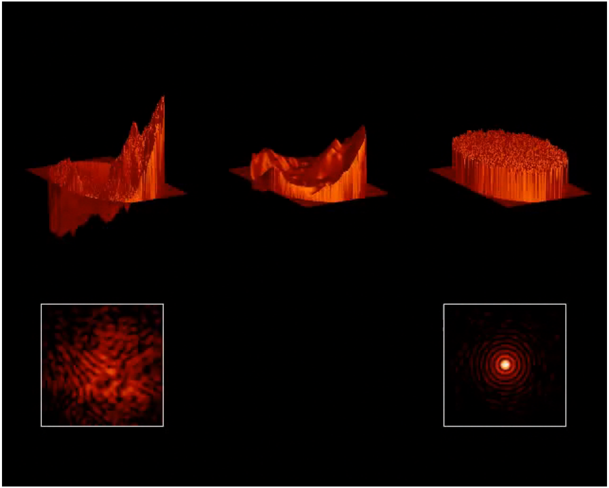

Orders of magnitude for wavefront sensing and control

Time constants

1. **From the ground:** Speckles de-correlate in a matter of minutes $\sim$ exposure time, the correction has to to occur during a science observing sequence.
2. **From space:** Speckles de-correlate in a matter of hours $\sim>$ exposure time, sensing can occur between observing sequences.

Contrast and non-common path

1. **From the ground:** Self-luminous Jupiters, contrast $\sim 10^7$.
2. **From space:** Reflected light earth-like planets, contrast $\sim 10^{10}$.
3. These constraints drive optical design: minimize the number of optics between the wavefront sensor and the science camera.

Wavefront sensing

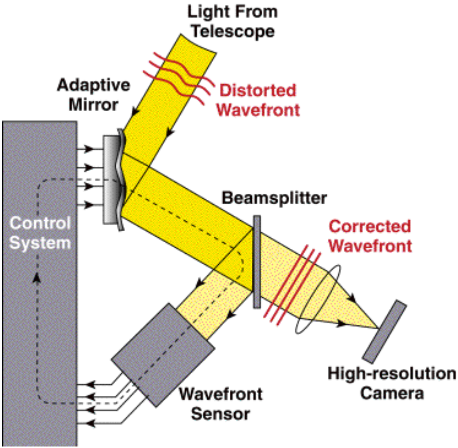

From Claire Max's lecture.

From space:

1. Because of the tight contrast constraint the sensing has to be done at the focal plane camera.
2. Science exposures can be used for the sensing.

From ground:

1. The sensing can happen a little before the science camera, some level of non common path is tolerable.
2. Because of the time constants the science exposures cannot be used for the sensing.

Underlying principle: interferences

The goal is to measure the wavefront but an images is the square modulus of the field

$$I = |a\, e^{i\phi}|^2$$

Solution: add a set of **known** wavefront disturbance in the plane of the camera

$$\begin{aligned} I_k &= |ae^{i\phi} + b_k e^{i\psi_k}|^2 \\ I_k &= a^2 + b_k^2 + 2ab_k \cos(\phi - \psi_k) \end{aligned}$$

Inverse problem

Solve for the ϕ, and a if needed, based on the know disturbances (b_k, ψ_k).

Depending on the configuration (b_k, ψ_k) might not be well known: modeling can play a crucial part in the wavefront sensing problem.

Trade-offs

Choosing the a wavefront sensing architecture is a trade-off between: the contrast constraint, time dependence constraint, and sensitivity to modeling.

Post Coronagraphic sensing

Wallace et al. (2009); Pueyo et al. (2010)

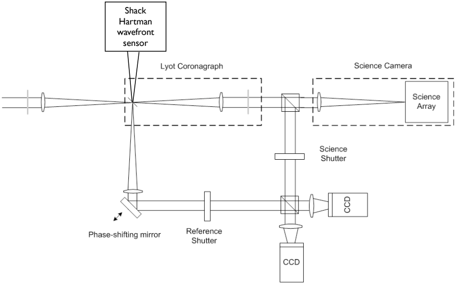

The light after the coronagraph is interfered with some of the light rejected by the coronagraph. The wavefront is retrieved using phase shifting interferomery.

If $(1+r)e^{i\phi}$ is the field **before** the coronagraph. Then the field **after** the coronagraph is $\sim r + i\phi$.

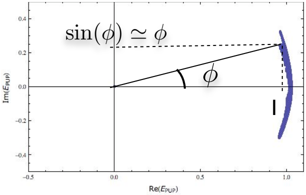

With $b_k e^{i\Psi_k} = b_0 e^{i(k-1)\frac{\pi}{2}}$ $k = 1, 2, 3, 4$ then:

$$\begin{aligned} \phi &\sim I_3 - I_1 \\ r &\sim I_4 - I_2 \end{aligned}$$

Post Coronagraphic sensing

Wallace et al. (2009); Pueyo et al. (2010)

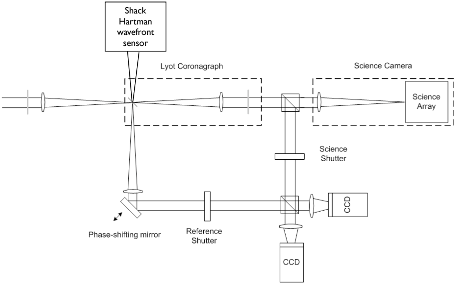

The light after the coronagraph is interfered with some of the light rejected by the coronagraph. The wavefront is retrieved using phase shifting interferomery.

If $(1+r)e^{i\phi}$ is the field **before** the coronagraph. Then the field **after** the coronagraph is $\sim r + i\phi$.

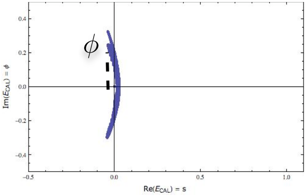

With $b_k e^{i\Psi_k} = b_0 e^{i(k-1)\frac{\pi}{2}}$ $k = 1, 2, 3, 4$ then:

$$\begin{aligned} \phi &\sim I_3 - I_1 \\ r &\sim I_4 - I_2 \end{aligned}$$

Post Coronagraphic sensing

Wallace et al. (2009); Pueyo et al. (2010)

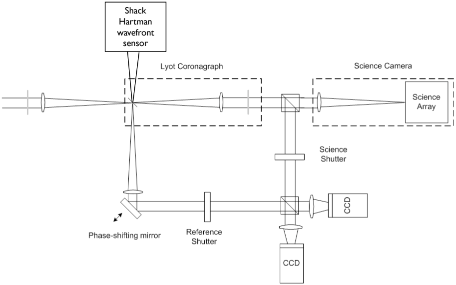

The light after the coronagraph is interfered with some of the light rejected by the coronagraph. The wavefront is retrieved using phase shifting interferomery.

Trade Offs

1. Sensing can occur during a science exposure: good for a ground based with short time constants.
2. Some optics between sensor and science camera: non-common path will limit contrast.
3. *If the interferometer is properly phased* then no model of the system is needed for reconstruction.

Interferometric measurement at the telescope

Palomar Hale Telescope

Interferometric measurement at the telescope

Courtesy of G. Vasisht

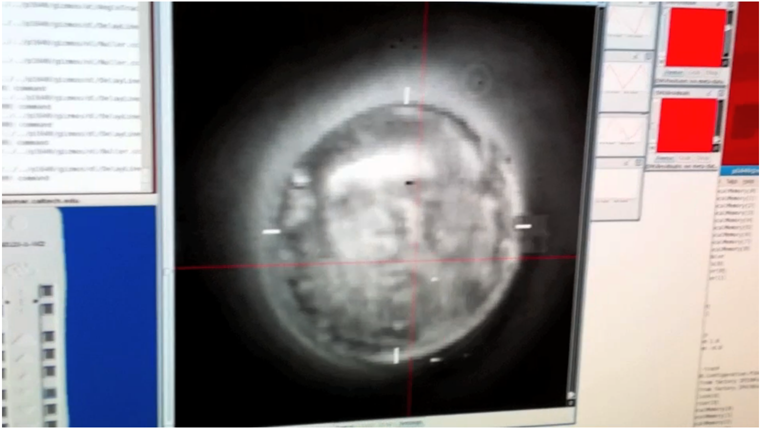

Interferometric measurement at the telescope

Courtesy of G. Vasisht

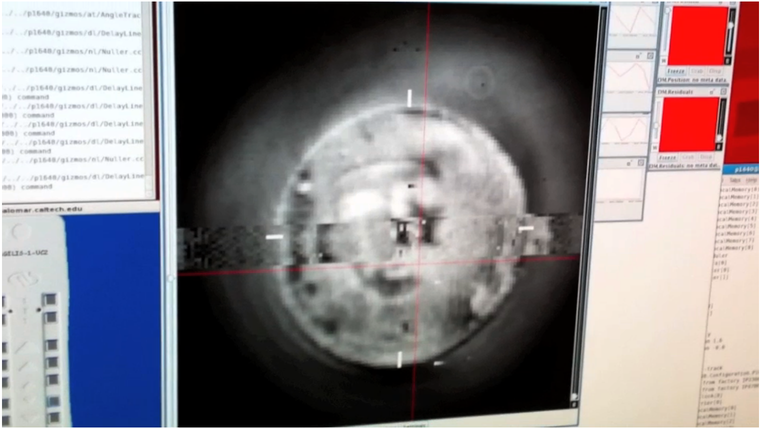

Interferometric measurement at the telescope

Courtesy of G. Vasisht

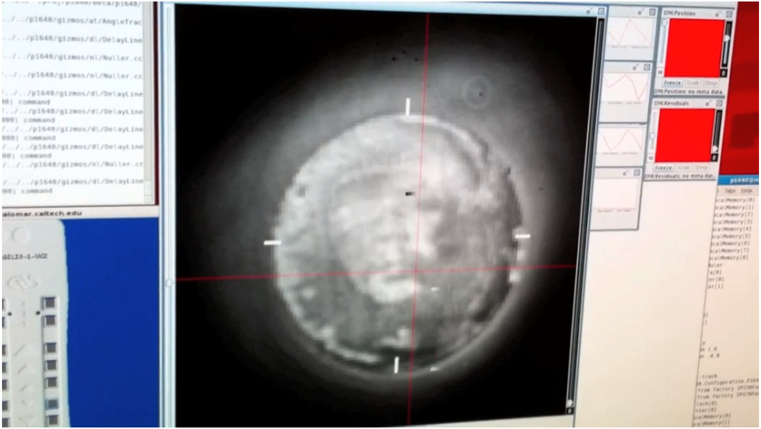

Interferometric measurement at the telescope

Courtesy of G. Vasisht

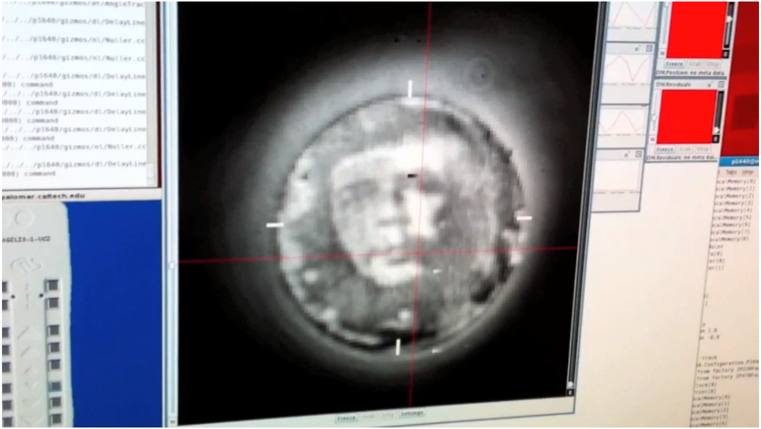

Interferometric measurement at the telescope

Courtesy of G. Vasisht

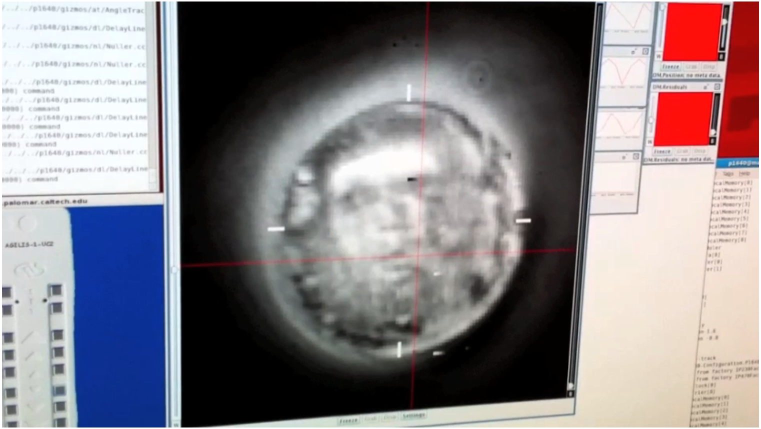

Focal plane sensing

Borde and Traub (2006); Give'on et al. (2007)

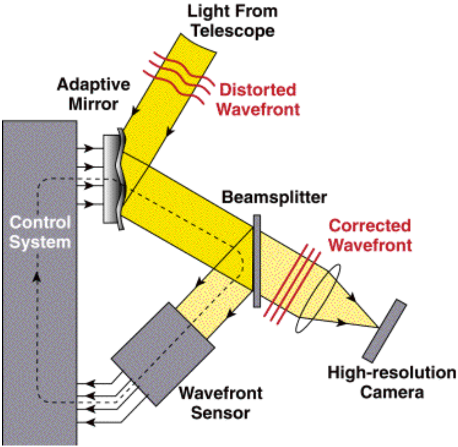

The light at the science camera is interfered with a tiny amount of light scattered by the DM.

If $Re(E_{Cam}) + iIm(E_{Cam})$ is the field **at** the science camera.

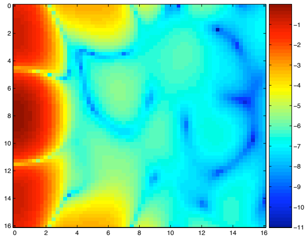

We choose shapes on the deformable mirror such that the additive disturbance at the science camera is $b_k e^{i\psi_k} = b_0 e^{i(k-1)\frac{\pi}{2}}$ $k = 1, 2, 3, 4$ then: Then:

$$\begin{aligned} Re(E_{Cam}) &\sim I_3 - I_1 \\ Im(E_{Cam}) &\sim I_4 - I_2 \end{aligned}$$

Focal plane sensing

Borde and Traub (2006); Give'on et al. (2007)

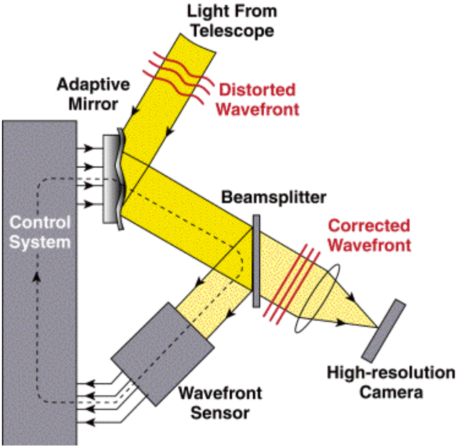

The light at the science camera is interfered with a tiny amount of light scattered by the DM.

If $Re(E_{Cam}) + iIm(E_{Cam})$ is the field **at** the science camera.

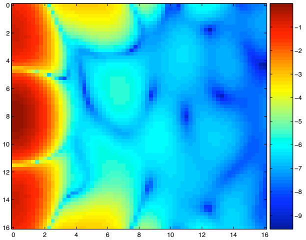

We choose shapes on the deformable mirror such that the additive disturbance at the science camera is $b_k e^{i\psi_k} = b_0 e^{i(k-1)\frac{\pi}{2}}$ $k = 1, 2, 3, 4$ then: Then:

$$Re(E_{Cam}) \sim I_3 - I_1$$
$$Im(E_{Cam}) \sim I_4 - I_2$$

Focal plane sensing

Borde and Traub (2006); Give'on et al. (2007)

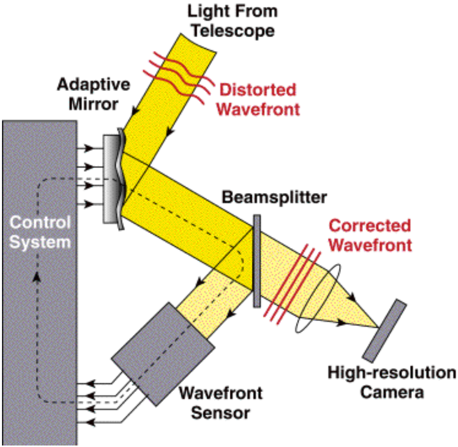

The light at the science camera is interfered with a tiny amount of light scattered by the DM.

If $Re(E_{Cam}) + iIm(E_{Cam})$ is the field **at** the science camera.

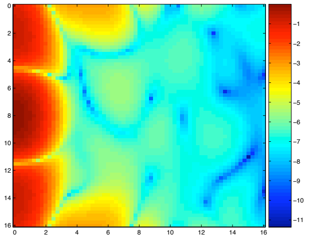

We choose shapes on the deformable mirror such that the additive disturbance at the science camera is $b_k e^{i\psi_k} = b_0 e^{i(k-1)\frac{\pi}{2}}$ $k = 1,2,3,4$ then: Then:

$$\begin{aligned} Re(E_{Cam}) &\sim I_3 - I_1 \\ Im(E_{Cam}) &\sim I_4 - I_2 \end{aligned}$$

Focal plane sensing

Borde and Traub (2006); Give'on et al. (2007)

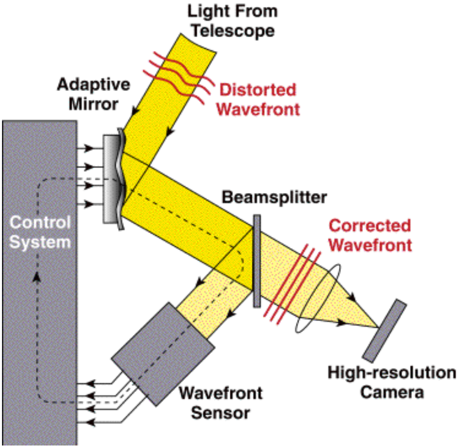

The light at the science camera is interfered with a tiny amount of light scattered by the DM.

If $Re(E_{Cam}) + iIm(E_{Cam})$ is the field **at** the science camera.

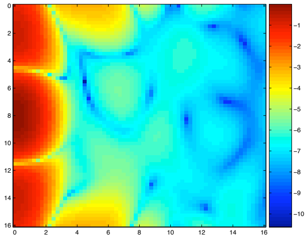

We choose shapes on the deformable mirror such that the additive disturbance at the science camera is $b_k e^{i\psi_k} = b_0 e^{i(k-1)\frac{\pi}{2}}$ $k = 1,2,3,4$ then: Then:

$$
\begin{aligned}
Re(E_{Cam}) &\sim I_3 - I_1 \\
Im(E_{Cam}) &\sim I_4 - I_2
\end{aligned}
$$

Focal plane sensing

Borde and Traub (2006); Give'on et al. (2007)

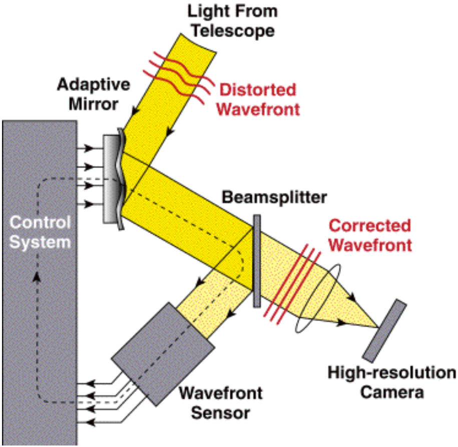

The light at the science camera is interfered with a tiny amount of light scattered by the DM.

Trade Offs

1. Sensing cannot occur during a science exposure: good for space based with long time constants.
2. No non-common path errors.
3. *Usually we do not know perfectly DM actuators to focal plane transfer function, sensitive to modeling.*

Focal plane sensing in practice

The field at the camera is a non-linear function of the voltages:

$$E_{cam}(\xi,\eta) = \mathscr{G}(V_1, ..., V_n, ..., V_N)$$

We discretize the focal plane in and linearize this function:

$$\begin{bmatrix} Re[E_{cam}(\xi_1,\eta_1)] \\ ... \\ Re[E_{cam}(\xi_p,\eta_q)] \\ ... \\ Re[E_{cam}(\xi_M,\eta_M)] \\ Im[E_{cam}(\xi_1,\eta_1)] \\ ... \\ Im[E_{cam}(\xi_p,\eta_q)] \\ ... \\ Im[E_{cam}(\xi_M,\eta_M)] \end{bmatrix} = \begin{bmatrix} \frac{\partial Re(\mathscr{G})}{\partial V_1}|(\xi_1,\eta_1) & ... & \frac{\partial Re(\mathscr{G})}{\partial V_N}|(\xi_1,\eta_1) \\ ... & .... & ... \\ ... & \frac{\partial Re(\mathscr{G})}{\partial V_n}|(\xi_p,\eta_q) & ... \\ ... & .... & ... \\ \frac{\partial Re(\mathscr{G})}{\partial V_1}|(\xi_1,\eta_1) & ... & \frac{\partial Re(\mathscr{G})}{\partial V_N}|(\xi_M,\eta_M) \\ \frac{\partial Im(\mathscr{G})}{\partial V_1}|(\xi_1,\eta_1) & ... & \frac{\partial Im(\mathscr{G})}{\partial V_N}|(\xi_1,\eta_1) \\ ... & .... & ... \\ ... & \frac{\partial Im(\mathscr{G})}{\partial V_n}|(\xi_p,\eta_q) & ... \\ ... & .... & ... \\ \frac{\partial Im(\mathscr{G})}{\partial V_1}|(\xi_1,\eta_1) & ... & \frac{\partial Im(\mathscr{G})}{\partial V_N}|(\xi_M,\eta_M) \end{bmatrix} \begin{bmatrix} V_1 \\ ... \\ V_n \\ ... \\ V_N \end{bmatrix}$$

Modelling tools

The modeling tools presented in the previous lecture are critical to compute a "G" matrix that is accurate enough.

Focal plane sensing in practice

$$
\begin{bmatrix}
Re[E_{cam}(\xi_1,\eta_1)] \\
\dots \\
Re[E_{cam}(\xi_p,\eta_q)] \\
\dots \\
Re[E_{cam}(\xi_M,\eta_M)] \\
Im[E_{cam}(\xi_1,\eta_1)] \\
\dots \\
Im[E_{cam}(\xi_p,\eta_q)] \\
\dots \\
Im[E_{cam}(\xi_M,\eta_M)]
\end{bmatrix}
=
\begin{bmatrix}
\frac{\partial Re(\mathscr{G})}{\partial V_1}|(\xi_1,\eta_1) & \dots & \frac{\partial Re(\mathscr{G})}{\partial V_N}|(\xi_1,\eta_1) \\
\dots & .... & \dots \\
\dots & \frac{\partial Re(\mathscr{G})}{\partial V_n}|(\xi_p,\eta_q) & \dots \\
\dots & .... & \dots \\
\frac{\partial Re(\mathscr{G})}{\partial V_1}|(\xi_1,\eta_1) & \dots & \frac{\partial Re(\mathscr{G})}{\partial V_N}|(\xi_M,\eta_M) \\
\frac{\partial Im(\mathscr{G})}{\partial V_1}|(\xi_1,\eta_1) & \dots & \frac{\partial Im(\mathscr{G})}{\partial V_N}|(\xi_1,\eta_1) \\
\dots & .... & \dots \\
\dots & \frac{\partial Im(\mathscr{G})}{\partial V_n}|(\xi_p,\eta_q) & \dots \\
\dots & .... & \dots \\
\frac{\partial Im(\mathscr{G})}{\partial V_1}|(\xi_1,\eta_1) & \dots & \frac{\partial Im(\mathscr{G})}{\partial V_N}|(\xi_M,\eta_M)
\end{bmatrix}
\begin{bmatrix}
V_1 \\ \dots \\ V_n \\ \dots \\ V_N
\end{bmatrix}
$$

Use the Deformable Mirror for diversity

1. We apply a set of probe voltages to the Deformable Mirror $\mathbf{V}_k = [V_1^k, ..., V_n^k ..., V_N^k \;\; k = 1, ..., N$

$$I_k = |E_{abb}|^2 + |G\mathbf{V}_k|^2 + 2 * Re(E_{abb} G\mathbf{V}_k)$$

2. We solve for $(Re[E_{abb}], Im[E_{abb}])$ for each point in the focal plane array.

Focal plane sensing as a detection method

Guyon et al. (2010)

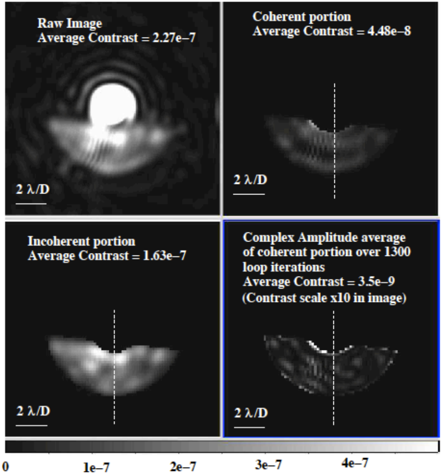

1. A planet is not coherent with the starlight.
2. It does not interfere with the light from the probes.
3. The signal from a planet does not appear in the coherent estimate.

Use wavefront sensing for detection

- In general any information on the structure of the aberration can be included in a detection algorithm.
- However the speckles are not fully deterministic, so this approach will be limited by photon noise.
- For this reason we try to suppress these speckles coherently.

Outline

1. Context
2. Wavefront sensing
3. Wavefront control
4. Conclusions

From the ground

In practice there are wavefront errors in the interferometer, amplitude error and coronagraphic leak can complicate the sensing:

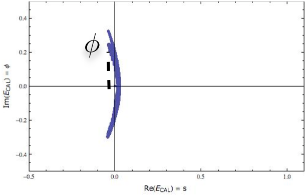

The $\phi \sim I_4 - I_2$ approximation is not valid.

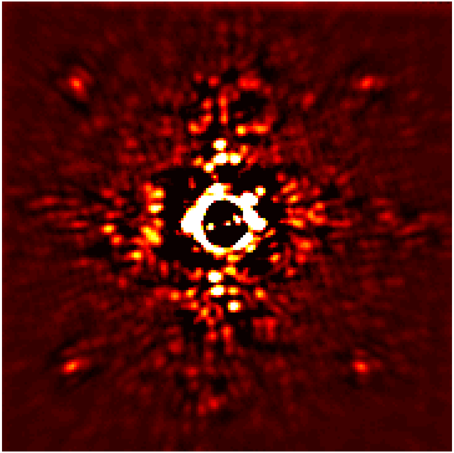

From the ground

In practice there are wavefront errors in the interferometer, amplitude error and coronagraphic leak can complicate the sensing:

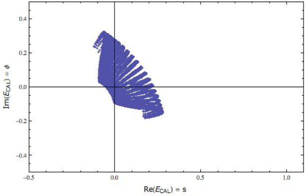

The $\phi \sim I_4 - I_2$ approximation is not valid.

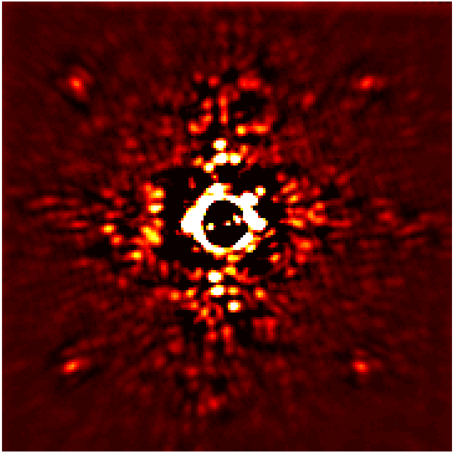

Model based correction

We measure G using the four step phase shifting interferometer.

1. We estimate $(Re[E_{Lyot}], Im[E_{Lyot}])$ using the four step phase shifting interferometer.
2. Since the Deformable Mirror can only create an imaginary field we seek to minimize the quadratic cost function:

$$||Im[E_{Lyot} - G\mathbf{V}]||^2$$

3. Since the coronagraph suppresses the low order modes, the linear problem associated with this minimization is ill-posed.
4. Using our "favorite regularization" we solve for the Deformable Mirror commands $\mathbf{V}$
5. We iterate.

P1640, Courtesy of G. Vasisht.

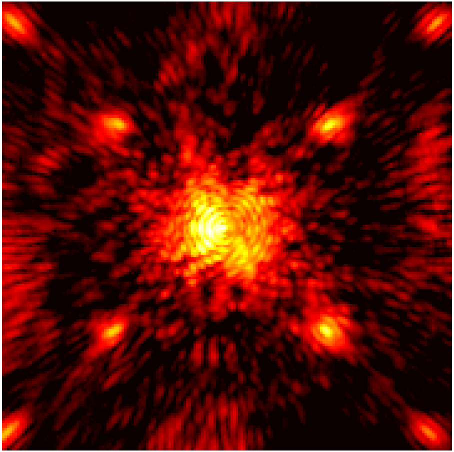

From the ground

P1640, Courtesy of G. Vasisht.

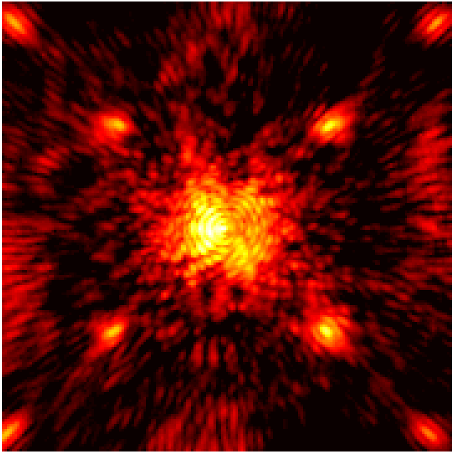

Residual speckles are amplitude

- Amplitude errors arise from reflectivity non uniformities and free space propagation of phase errors, Pueyo and Kasdin (2007).
- Deformable Mirror is a phase only actuator.
- Even if the interferometer can measure amplitude the Deformable Mirror cannot "fully" correct such errors.

From the ground

P1640, Courtesy of G. Vasisht.

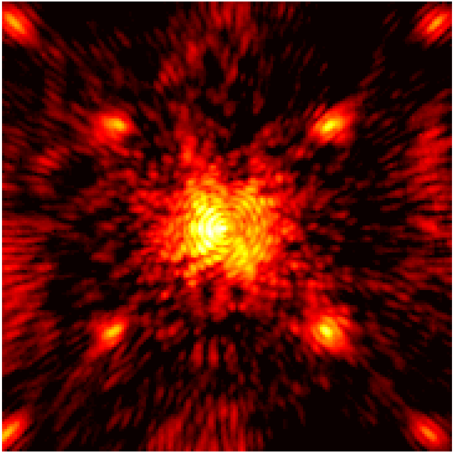

Residual speckles are amplitude

- Amplitude errors arise from reflectivity non uniformities and free space propagation of phase errors, Pueyo and Kasdin (2007).
- Deformable Mirror is a phase only actuator.
- Even if the interferometer can measure amplitude the Deformable Mirror cannot "fully" correct such errors.

Half dark hole, theory

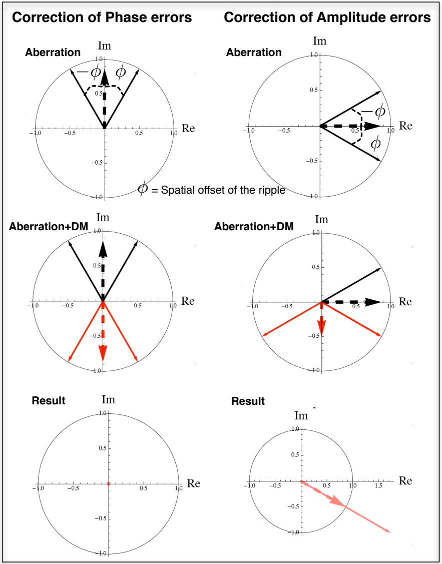

The field after the coronagraph or at the image plane can be written under the linear approximation as:

$$(1+r)e^{i\phi} \simeq 1 + r + i\phi$$

- Amplitude in the plane of the Deformable Mirror creates an hermitian pattern in the image plane.
- Phase in the plane of the Deformable Mirror creates an anti-hermitian pattern in the image plane.
- Phase on the Deformable Mirror can correct for half of the amplitude errors
- This leads to a dark hole only on one side of the optical axis.

Model based correction

We calculate G using a high fidelity model.

1. We estimate $(Re[E^{\lambda_p}_{abb}], Im[E^{\lambda_p}_{abb}])$ for a series of wavelength λ_p in the bandpass.
2. Since we minimize the cost function *only on one side of the image plane*:

$$\sum_p ||E^{\lambda_p}_{abb} - G^{\lambda_p}\mathbf{V}]||^2$$

3. Since the coronagraph suppresses the low order modes, the linear problem associated with this minimization is ill-posed.
4. Using our "favorite regularization" we solve for the Deformable Mirror commands $\mathbf{V}$
5. We iterate.

High Contrast Imaging Testbed, JPL

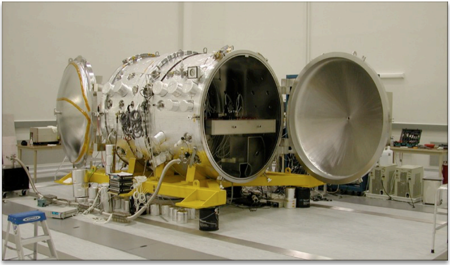

Borde and Traub (2006); Give'on et al. (2007)

Model based correction

We calculate G using a high fidelity model.

1. We estimate $(Re[E_{abb}^{\lambda_p}], Im[E_{abb}^{\lambda_p}])$ for a series of wavelength λ_p in the bandpass.
2. Since we minimize the cost function *only on one side of the image plane*:

$$\sum_p ||E_{abb}^{\lambda_p} - G^{\lambda_p}\mathbf{V}]||^2$$

3. Since the coronagraph suppresses the low order modes, the linear problem associated with this minimization is ill-posed.
4. Using our "favorite regularization" we solve for the Deformable Mirror commands **V**
5. We iterate.

Courtesy of A. Give'on

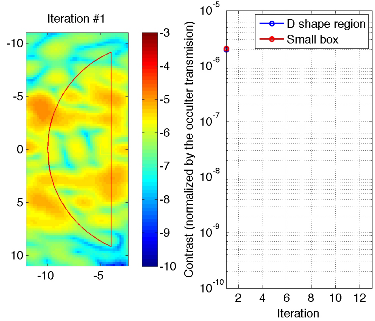

Borde and Traub (2006); Give'on et al. (2007)

Model based correction

We calculate G using a high fidelity model.

1. We estimate $(Re[E_{abb}^{\lambda_p}], Im[E_{abb}^{\lambda_p}])$ for a series of wavelength λ_p in the bandpass.
2. Since we minimize the cost function *only on one side of the image plane*:

$$\sum_p ||E_{abb}^{\lambda_p} - G^{\lambda_p}\mathbf{V}]||^2$$

3. Since the coronagraph suppresses the low order modes, the linear problem associated with this minimization is ill-posed.
4. Using our "favorite regularization" we solve for the Deformable Mirror commands $\mathbf{V}$
5. We iterate.

Courtesy of A. Give'on

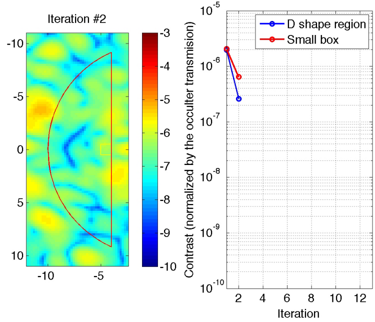

Borde and Traub (2006); Give'on et al. (2007)

Half Dark hole correction

Model based correction

We calculate G using a high fidelity model.

1. We estimate $(Re[E_{abb}^{\lambda_p}], Im[E_{abb}^{\lambda_p}])$ for a series of wavelength λ_p in the bandpass.
2. Since we minimize the cost function *only on one side of the image plane*:

$$\sum_p ||E_{abb}^{\lambda_p} - G^{\lambda_p}\mathbf{V}]||^2$$

3. Since the coronagraph suppresses the low order modes, the linear problem associated with this minimization is ill-posed.
4. Using our "favorite regularization" we solve for the Deformable Mirror commands $\mathbf{V}$
5. We iterate.

Courtesy of A. Give'on

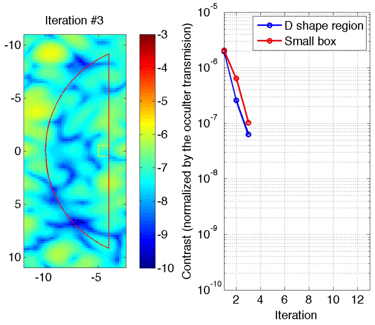

Borde and Traub (2006); Give'on et al. (2007)

Model based correction

We calculate G using a high fidelity model.

1. We estimate $(Re[E_{abb}^{\lambda_p}], Im[E_{abb}^{\lambda_p}])$ for a series of wavelength λ_p in the bandpass.
2. Since we minimize the cost function *only on one side of the image plane*:
$$\sum_p ||E_{abb}^{\lambda_p} - G^{\lambda_p}\mathbf{V}]||^2$$
3. Since the coronagraph suppresses the low order modes, the linear problem associated with this minimization is ill-posed.
4. Using our "favorite regularization" we solve for the Deformable Mirror commands $\mathbf{V}$
5. We iterate.

Courtesy of A. Give'on

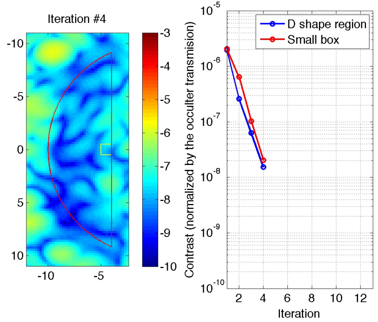

Borde and Traub (2006); Give'on et al. (2007)

Model based correction

We calculate G using a high fidelity model.

1. We estimate $(Re[E^{\lambda_p}_{abb}], Im[E^{\lambda_p}_{abb}])$ for a series of wavelength λ_p in the bandpass.
2. Since we minimize the cost function *only on one side of the image plane*:

$$\sum_p ||E^{\lambda_p}_{abb} - G^{\lambda_p}\mathbf{V}]||^2$$

3. Since the coronagraph suppresses the low order modes, the linear problem associated with this minimization is ill-posed.
4. Using our "favorite regularization" we solve for the Deformable Mirror commands $\mathbf{V}$
5. We iterate.

Courtesy of A. Give'on

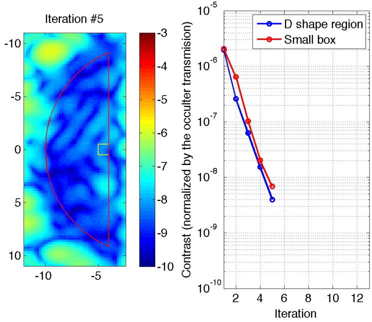

Borde and Traub (2006); Give'on et al. (2007)

Model based correction

We calculate G using a high fidelity model.

1. We estimate $(Re[E_{abb}^{\lambda_p}], Im[E_{abb}^{\lambda_p}])$ for a series of wavelength λ_p in the bandpass.
2. Since we minimize the cost function *only on one side of the image plane*:

$$\sum_p ||E_{abb}^{\lambda_p} - G^{\lambda_p}\mathbf{V}]||^2$$

3. Since the coronagraph suppresses the low order modes, the linear problem associated with this minimization is ill-posed.
4. Using our “favorite regularization” we solve for the Deformable Mirror commands $\mathbf{V}$
5. We iterate.

Courtesy of A. Give’on

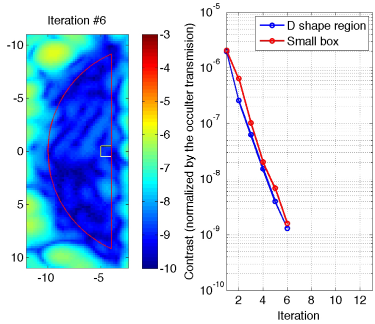

Borde and Traub (2006); Give’on et al. (2007)

Model based correction

We calculate G using a high fidelity model.

1. We estimate $(Re[E_{abb}^{\lambda_p}], Im[E_{abb}^{\lambda_p}])$ for a series of wavelength λ_p in the bandpass.
2. Since we minimize the cost function *only on one side of the image plane*:

$$\sum_p ||E_{abb}^{\lambda_p} - G^{\lambda_p}\mathbf{V}]||^2$$

3. Since the coronagraph suppresses the low order modes, the linear problem associated with this minimization is ill-posed.
4. Using our "favorite regularization" we solve for the Deformable Mirror commands $\mathbf{V}$
5. We iterate.

Courtesy of A. Give'on

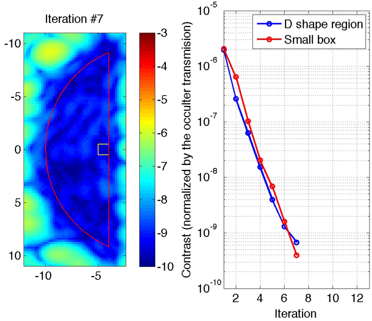

Borde and Traub (2006); Give'on et al. (2007)

Model based correction

We calculate G using a high fidelity model.

1. We estimate $(Re[E_{abb}^{\lambda_p}], Im[E_{abb}^{\lambda_p}])$ for a series of wavelength λ_p in the bandpass.
2. Since we minimize the cost function *only on one side of the image plane*:

$$\sum_p ||E_{abb}^{\lambda_p} - G^{\lambda_p}\mathbf{V}]||^2$$

3. Since the coronagraph suppresses the low order modes, the linear problem associated with this minimization is ill-posed.
4. Using our "favorite regularization" we solve for the Deformable Mirror commands $\mathbf{V}$
5. We iterate.

Courtesy of A. Give'on

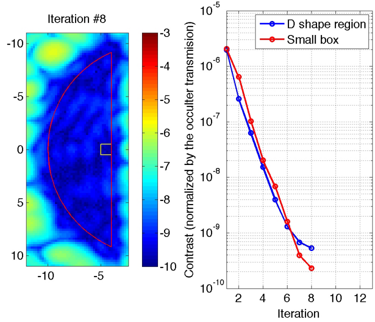

Borde and Traub (2006); Give'on et al. (2007)

Model based correction

We calculate G using a high fidelity model.

1. We estimate $(Re[E_{abb}^{\lambda_p}], Im[E_{abb}^{\lambda_p}])$ for a series of wavelength λ_p in the bandpass.
2. Since we minimize the cost function *only on one side of the image plane*:

$$\sum_p ||E_{abb}^{\lambda_p} - G^{\lambda_p}\mathbf{V}]||^2$$

3. Since the coronagraph suppresses the low order modes, the linear problem associated with this minimization is ill-posed.
4. Using our "favorite regularization" we solve for the Deformable Mirror commands $\mathbf{V}$
5. We iterate.

Courtesy of A. Give'on

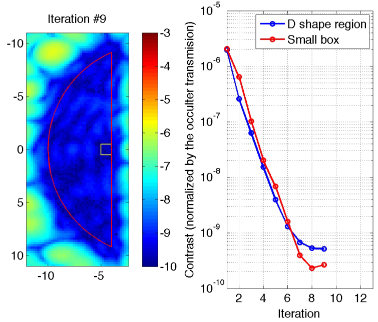

Borde and Traub (2006); Give'on et al. (2007)

Model based correction

We calculate G using a high fidelity model.

1. We estimate $(Re[E^{\lambda_p}_{abb}], Im[E^{\lambda_p}_{abb}])$ for a series of wavelength λ_p in the bandpass.
2. Since we minimize the cost function *only on one side of the image plane*:

$$\sum_p ||E^{\lambda_p}_{abb} - G^{\lambda_p}\mathbf{V}]||^2$$

3. Since the coronagraph suppresses the low order modes, the linear problem associated with this minimization is ill-posed.
4. Using our "favorite regularization" we solve for the Deformable Mirror commands **V**
5. We iterate.

Courtesy of A. Give'on

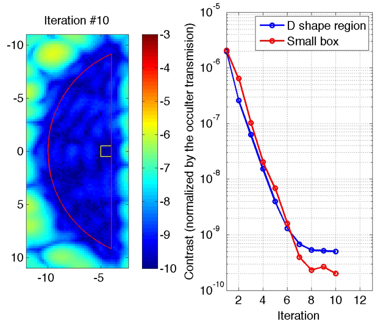

Borde and Traub (2006); Give'on et al. (2007)

Model based correction

We calculate G using a high fidelity model.

1. We estimate $(Re[E_{abb}^{\lambda_p}], Im[E_{abb}^{\lambda_p}])$ for a series of wavelength λ_p in the bandpass.
2. Since we minimize the cost function *only on one side of the image plane*:

$$\sum_p ||E_{abb}^{\lambda_p} - G^{\lambda_p}\mathbf{V}]||^2$$

3. Since the coronagraph suppresses the low order modes, the linear problem associated with this minimization is ill-posed.
4. Using our “favorite regularization” we solve for the Deformable Mirror commands $\mathbf{V}$
5. We iterate.

Courtesy of A. Give'on

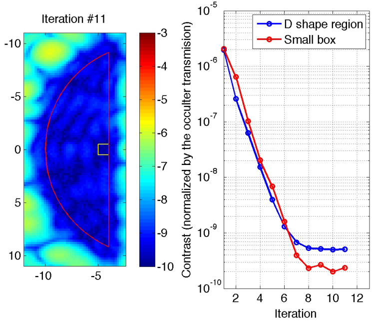

Borde and Traub (2006); Give'on et al. (2007)

Model based correction

We calculate G using a high fidelity model.

1. We estimate $(Re[E^{\lambda_p}_{abb}], Im[E^{\lambda_p}_{abb}])$ for a series of wavelength λ_p in the bandpass.
2. Since we minimize the cost function *only on one side of the image plane*:

$$\sum_p ||E^{\lambda_p}_{abb} - G^{\lambda_p}\mathbf{V}]||^2$$

3. Since the coronagraph suppresses the low order modes, the linear problem associated with this minimization is ill-posed.
4. Using our "favorite regularization" we solve for the Deformable Mirror commands $\mathbf{V}$
5. We iterate.

Courtesy of A. Give'on

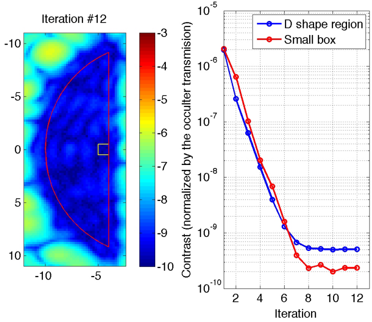

Borde and Traub (2006); Give'on et al. (2007)

Model based correction

We calculate G using a high fidelity model.

1. We estimate $(Re[E_{abb}^{\lambda_p}], Im[E_{abb}^{\lambda_p}])$ for a series of wavelength λ_p in the bandpass.
2. Since we minimize the cost function *only on one side of the image plane*:

$$\sum_p ||E_{abb}^{\lambda_p} - G^{\lambda_p}\mathbf{V}]||^2$$

3. Since the coronagraph suppresses the low order modes, the linear problem associated with this minimization is ill-posed.
4. Using our "favorite regularization" we solve for the Deformable Mirror commands $\mathbf{V}$
5. We iterate.

Courtesy of A. Give'on

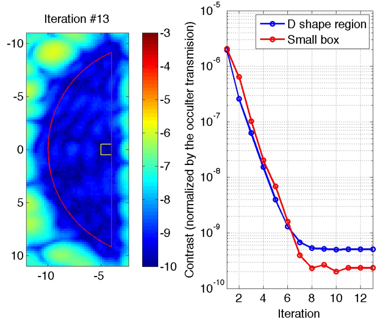

Borde and Traub (2006); Give'on et al. (2007)

Model based correction

We calculate G using a high fidelity model.

1. We estimate $(Re[E_{abb}^{\lambda_p}], Im[E_{abb}^{\lambda_p}])$ for a series of wavelength λ_p in the bandpass.
2. Since we minimize the cost function *only on one side of the image plane*:

$$\sum_p ||E_{abb}^{\lambda_p} - G^{\lambda_p}\mathbf{V}]||^2$$

3. Since the coronagraph suppresses the low order modes, the linear problem associated with this minimization is ill-posed.
4. Using our "favorite regularization" we solve for the Deformable Mirror commands $\mathbf{V}$
5. We iterate.

Courtesy of A. Give'on

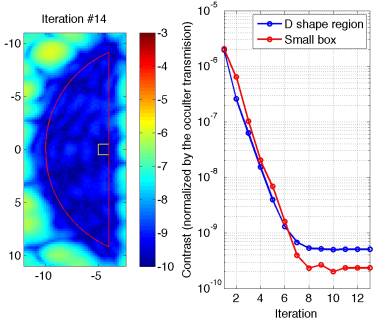

Borde and Traub (2006); Give'on et al. (2007)

Model based correction

We calculate G using a high fidelity model.

1. We estimate $(Re[E_{abb}^{\lambda_p}], Im[E_{abb}^{\lambda_p}])$ for a series of wavelength λ_p in the bandpass.
2. Since we minimize the cost function *only on one side of the image plane*:

$$\sum_p ||E_{abb}^{\lambda_p} - G^{\lambda_p}\mathbf{V}]||^2$$

3. Since the coronagraph suppresses the low order modes, the linear problem associated with this minimization is ill-posed.
4. Using our "favorite regularization" we solve for the Deformable Mirror commands $\mathbf{V}$
5. We iterate.

Courtesy of A. Give'on

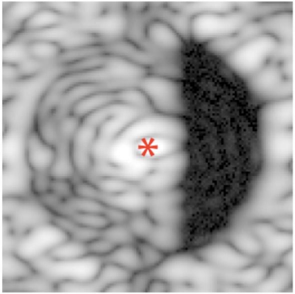

Borde and Traub (2006); Give'on et al. (2007)

Use two deformable mirrors in series

One of the deformable mirrors is not placed at a conjugate of the pupil.

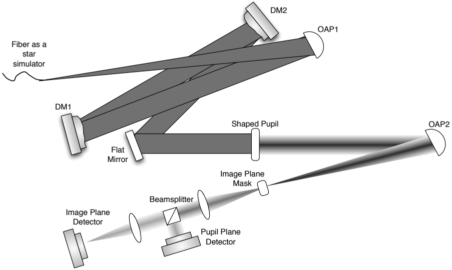

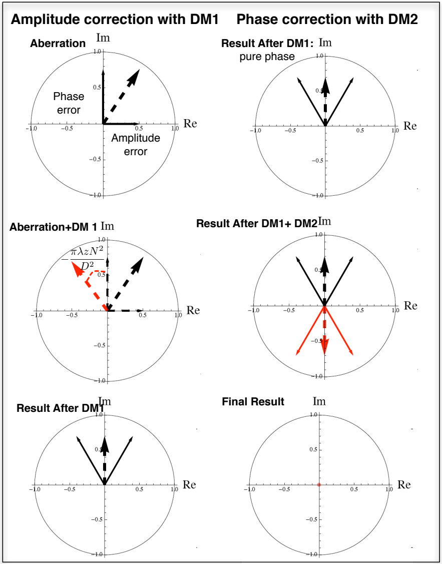

Weak coupling

The coupling between phase and amplitude is weak, a large phase deformation is needed to create a small amplitude term.

Model based correction

We calculate G_{DM1} and G_{DM2} using a high fidelity model and concatenate then in a $2N$ dimensional G.

1. We estimate $(Re[E_{abb}^{\lambda_p}], Im[E_{abb}^{\lambda_p}])$ for a series of wavelength λ_p in the bandpass.
2. We minimize the cost function *only on both sides of the image plane*:

$$\sum_p ||E_{abb}^{\lambda_p} - G^{\lambda_p}\mathbf{V}||^2 \qquad (1)$$

3. Since the coronagraph suppresses the low order modes, the linear problem associated with this minimization is ill-posed.
4. We proceed through a careful inversion that seeks to minimize the surface Deformations of the DM to circumvent the weak coupling.
5. We iterate.

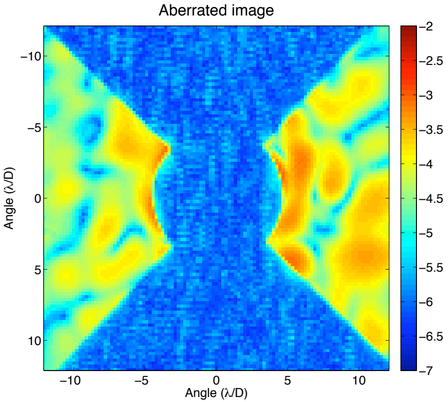

Pueyo et al. (2009)

Two Deformable Mirrors correction

Correction methodology

- At a given iteration we choose a target contrast.
- We estimate $(Re[E_{abb}^{\lambda_p}], Im[E_{abb}^{\lambda_p}])$ for a series of wavelength λ_p in the bandpass.
- **Mininize** $\sum_k |V_k^{(1)}|^2 + |V_k^{(2)}|^2$ **under the constraint** $\sum_p I^{\lambda_p} < 10^C$: use the two DMs to correct the amplitude part.
- In this case the intensity in the Dark Hole is still a quadratic form

$$\begin{aligned} I^{\lambda_p} &= \sum_p \left(\frac{2\pi\lambda_0}{\lambda_p}\right)^2 [\mathbf{V}_1\ \mathbf{V}_2] \begin{bmatrix} M_{11}^{(\lambda_p)} & M_{12}^{(\lambda_p)} \\ M_{12}^{(\lambda_p)} & M_{22}^{(\lambda_p)} \end{bmatrix} [X_1\ X_2]^T \\ &+ 2\frac{2\pi\lambda_0}{\lambda_p}[\mathbf{V}_1\ \mathbf{V}_2].\Im([b_1^{(\lambda_p)}\ b_2^{(\lambda_p)}]^T) \end{aligned}$$

  Where the M's are the self correlation of the G^{λ_p}'s with themselves and b's are the correlation of the G^{λ_p}'s with $(Re[E_{abb}^{\lambda_p}], Im[E_{abb}^{\lambda_p}])$
- Once the correction has been applied we iterate to a lower contrast target. This ensures convergence.

Two Deformable Mirrors correction

High Contrast Imaging Laboratory, Princeton

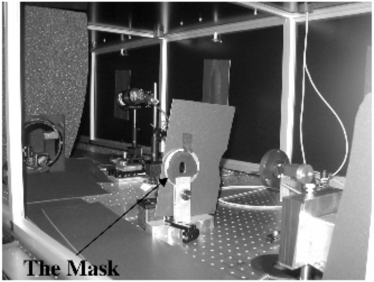

Two Deformable Mirrors correction

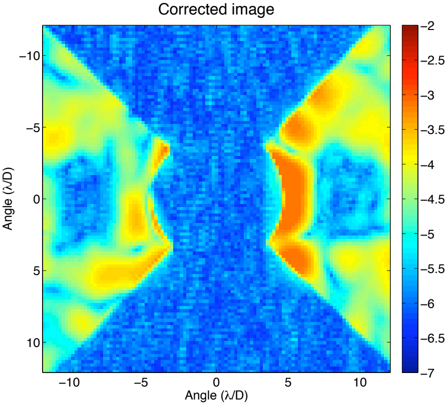

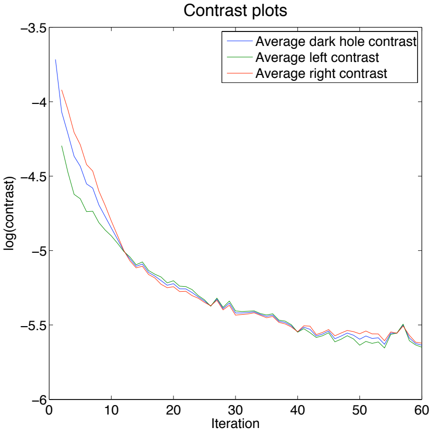

Pueyo et al. (2009)

Convergence is slower because of the extra care with which the weak coupling was treated.

Outline

1. Context

2. Wavefront sensing

3. Wavefront control

4. Conclusions

Wrap up

Wavefront correction changes chromaticity

$$
\begin{aligned}
I^{\lambda_p} &= \sum_p \left(\frac{2\pi\lambda_0}{\lambda_p}\right)^2 [\mathbf{V}_1\ \mathbf{V}_2] \begin{bmatrix} M_{11}^{(\lambda_p)} & M_{12}^{(\lambda_p)} \\ M_{12}^{(\lambda_p)} & M_{22}^{(\lambda_p)} \end{bmatrix} [X_1\ X_2]^T \\
&+ 2\frac{2\pi\lambda_0}{\lambda_p}[\mathbf{V}_1\ \mathbf{V}_2].\Im([b_1^{(\lambda_p)}\ b_2^{(\lambda_p)}]^T)
\end{aligned}
$$

Whether one or two Deformable mirrors are used, various weights are given to wavelength in the correction.
The wavefront control makes the speckles smaller but much more chromatic and thus a lot harder to model in order use chromaticity priors for detection.

Wavefront sensing is an "optical solution" of the detection problem

For focal plane wavefront sensing: if the speckles can be perfectly estimated at a given contrast, then a planet can be detected at that contrast.
For non focal plane sensing: the estimate can be used to inform the detection algorithm about the potential PSF structures due to aberrations.

For Further Reading

Crepp, J. R. and Pueyo, L. and Brenner, D. and Oppenheimer, B. R. and Zimmerman, N. and Hinkley, S. and Parry, I. and King, D. and Vasisht, G. and Beichman, C. and Hillenbrand, L. and Dekany, R. and Shao, M. and Burruss, R. and Roberts, L. C. and Bouchez, A. and Roberts, J. and Soummer, R.. 2011, ApJ, 729, 132-+

J. Kent Wallace , Rick Burruss , Laurent Pueyo and Remi Soummer, Chris Shelton, Randall Bartos, Felipe Fregoso, Bijan Nemati, Paul Best, John Angione, Procs SPIE 7440, 2009

Laurent Pueyo, Kent Wallace , Mitchell Troy, Rick Burruss, Bruce Macintosh, Remi Soummer, Procs SPIE 7736, 2010

Bord, P. J. and Traub, W. A., 2006, ApJ, 638, 488-498

Amir Give'on, Ruslan Belikov, Stuart Shaklan , Jeremy Kasdin, 2007, Optics Express, Vol 15, Number 19, 12338–12343

Guyon, O., Pluzhnik, E., Martinache, F., Totems, J., Tanaka, S., Matsuo, T., Blain, C., Belikov, R. 2010, PASP, 122, 72-84

Pueyo, L. and Kasdin, N. J., 2007, ApJ, 666, 609-625

Laurent Pueyo, Jason Kay, N. Jeremy Kasdin, Tyler Groff , Michael McElwain, Amir Give'on, Ruslan Belikov, 2009, Applied Optics, Vol 48, Num 32, 6296–6312